

---

# On Transferring Expert Knowledge from Tabular Data to Images Supplementary Material

---

Anonymous Author(s)

Affiliation

Address

email

## 1 A Experiment Details

### 2 A.1 Dataset Details

3 The datasets used in our experiments are MFEAT [13], Data Visual Marketing (DVM) [6],  
4 SUNAttribute [11], CelebA [8], PetFinder-adoption, PetFinder-pawpularity and Avito.

5 **MFEAT.** This dataset consists of features of handwritten numerals ('0'-'9') extracted from a collec-  
6 tion of Dutch utility maps. 200 patterns per class (for a total of 2,000 patterns) have been digitized in  
7 binary images. These digits are represented in terms of the following six feature sets. We use only 76  
8 fourier coefficients of the character shapes and 6 morphological features for tabular data. The image  
9 modality is reconstructed from 240 pixel averages of images from  $2 \times 3$  windows.

10 **DVM.** DVM dataset aims to facilitate business related research and applications in automotive  
11 industry such as car appearance design, consumer analytics and sales modeling. The dataset contains  
12 car images, model specifications and sales information about 899 car models that have been sold in  
13 the UK market over the last 20 years. which comprises two data parts: the image data and the table  
14 data. The former contains 1,451,784 car images that have been deliberately cleaned and organized.  
15 While the latter includes six CSV tables that cover the non-visual attributes such as brand, price,  
16 sales, etc. Different from MMCL, only the new version DVM dataset is available [3]. We pair this  
17 tabular data with a single random image from each advertisement, yielding a dataset of 70,580 train  
18 pairs, 17,645 validation pairs, and 88,226 test pairs. Car models with less than 700 samples were  
19 removed, resulting in 129 target classes, classification task. There are total of 13 numerical variables  
20 and 3 categorical variables in this dataset. We expect that under the guidance of tabular data, images  
21 can learn more knowledge and make classification better.

22 The DVM dataset utilized in the original paper is an earlier version, and unfortunately, we don't have  
23 access to the dataset after the official update. This discrepancy in dataset versions may introduce  
24 variations in the data distribution and characteristics. Specifically, all the images are resized to  
25 300x300 resolutions; Segment results are no longer provided directly; Image data of 2019 registered  
26 car models is added and the non-visual feature data is updated to 2020.

27 We follow the steps in [3] in Section 4.1 to preprocess the data. In detail, the car models with less  
28 than 700 samples were removed, resulting in 129 target classes. This process ensures that the amount  
29 of data remain largely consistent with [3].

30 Lastly, to maintain uniformity and facilitate fair comparisons, we employed a fixed batch size of 64  
31 across all methods, whereas the original paper employed a larger 512. Additionally, we conducted  
32 MMCL method on our dataset with a batch size of 512. The result was 0.8869/0.9070. This is still  
33 somewhat different from the values reported in [3] and performs worse than our method 0.9207 with  
34 a batch size of 512.

35 Furthermore, we conducted a comparison of GPU usage with batch size 64. Our method uses 8  
36 GB of memory while theirs uses 20 GB. The results revealed that the MMCL method remains  
37 resource-intensive. Conversely, our method achieves superior performance with lower computational  
38 costs, further highlighting the efficiency of our approach.

39 **SUNAttribute.** SUNAttribute annotates 20 scenes from each of the 717 SUN categories. Each scene  
40 has 102 attributes and each attribute will have multiple annotations. For simplicity, we divide each  
41 attribute into zero and one and our goal is to predict whether a scene is an open space, which is a  
42 binary classification task. The dataset contains 14,340 images and the corresponding table feature,  
43 each attribute of the table feature represents a scene and takes the value of 1 if the attribute is present  
44 in the image. we use 8 : 1 : 1 to divide the training set, validation set, and testing set. There are total  
45 of 101 categorical variables in this dataset.

46 **CelebA.** is the abbreviation of CelebFaces Attribute, meaning celebrity face attribute dataset, which  
47 contains 202,599 face images of 10,177 celebrities, each image is well marked with features,  
48 including 40 attribute markers such as Big\_Nose. We use Attractive as the label, which is a binary  
49 classification task. We use 8 : 1 : 1 to divide the training set, validation set, and testing set. There are  
50 total of 39 categorical variables in this dataset. We expect to introduce more detailed face information  
51 in the table, allowing the image to perform better on downstream tasks.

52 **PetFinder-adoption.** Animal adoption rates are strongly correlated to the metadata associated with  
53 their online profiles, such as descriptive text and photo characteristics. This dataset comes from  
54 a kaggle competition where the task is to predict the speed at which a pet is adopted, which is a  
55 five-class classification task. There are total of 10 numerical variables and 14 categorical variables in  
56 this dataset. Tabular data contains information about the pet such as the type and vaccination status.  
57 We also use the same division for the dataset.

58 **PetFinder-pawpularity.** This dataset also comes from a kaggle competition where the task was to  
59 predict the popularity of a pet based on that pet’s profile and photo, which is a regression task. Each  
60 pet photo is labeled with the value of 1 (Yes) or 0 (No) for each of features. For example, “Face”  
61 represents whether the face of the pet in the picture is frontal. There are 12 categorical variables in  
62 tabular data.

63 **Avito.** Avito, Russia’s largest classified advertisements website, is deeply familiar with this problem.  
64 Sellers on their platform sometimes feel frustrated with both too little demand (indicating something  
65 is wrong with the product or the product listing) or too much demand (indicating a hot item with a  
66 good description was underpriced). This dataset is challenging you to predict demand for an online  
67 advertisement based on its full description, its context and historical demand for similar ads in similar  
68 contexts. The target deal\_probability can be any float from zero to one. It’s also a regression task.  
69 There are total of 2 numerical variables such as and 11 categorical variables such as in this dataset.






## 70 A.2 Training Details

71 We use ResNet50 with weight pretrained on ImageNet-1k [12] as image feature extractor for all  
72 methods mentioned in this paper. The classifier is built from an MLP with one hidden layer of size  
73 1024.

74 For baseline methods, the numerical tabular data fields are standardized using z-score normaliza-  
75 tion with a mean value of 0 and standard deviation of 1. For our method CHARMS, we use FT-  
76 Transformer [2] to get the embedding of tabular data, which can process continuous and categorical  
77 variables separately.

- 78 • **KD [5]:** For KD method, we search the temperatures in  $\{1.0, 2.0, 4.0, 6.0, 8.0\}$  and  $\lambda$  in  
79  $\{0.2, 0.4, 0.6, 0.8\}$ .
- 80 • **KD-Fou:** This means that we use only 76 fourier coefficients of the character shapes features  
81 when training the teacher network.
- 82 • **KD-Mor:** This means that we use only 6 morphological features when training the teacher  
83 network, which can be revealed in images.
- 84 • **FMR [17]:** We set ten percent of the fixed features to be knockdown in each epoch in FMR  
85 method. The fixed feature classifier is a linear connection between tabular data and the  
86 corresponding image.

Table 1: Introduction to the dataset. Here we introduce image data and tabular data in each dataset, and numerical and categorical variables are introduced separately in the tabular data. An example is given for each dataset.

Dataset	Numerical Attribute	Categorical Attribute	Image
MFEAT	Fourier coefficient_1 0.13839	-	
DVM	Length 4865.0	Fuel_type 9	
SUNAttribute	-	Warm 1	
CelebA	-	Big_Nose 0	
PetFinder-adoption	Fee 100	Type 0	
PetFinder-pawpularity	-	Focus 0	
Avito	Price 1290	Category_name 4	

- 87
- 88
- 89
- 90
- 91
- 92
- 93
- 94
- 95
- 96
- 97
- **MFH [16]:** For MFH method, we set modality general decisive information according to the feature ranking algorithm. The number of the features is fifty percent of that for all features.
  - **MMCL [3]:** The same parameters are set for MMCL method according to [3]. We use the frozen version after pretrain and only train the classifier for downstream task.
  - **CHARMS:** For FT-Transformer, the number of Transformer blocks is set to 2. We use the K-Means method to cluster the representations obtained by ResNet50 and  $n\_cluster$  is 40. Embedding dimension  $E$  is set according to the data distribution. Adam optimizer with weight decay is used to train the models. We choose to update cost matrix every 5 epochs, striking a balance between updating them without stable knowledge and minimizing the computational burden. However, we continuously update  $\phi$  throughout the training process to enhance the representation.

Table 2: Comparisons with baseline methods on DVM, SUN, CelebA, Adoption, Pawpularity, and Avito datasets on five random seeds.

	DVM $\uparrow$	SUN $\uparrow$	CelebA $\uparrow$	Adoption $\uparrow$	Pawpularity $\downarrow$	Avito $\downarrow$
LGB	0.9748 $\pm$ 0.0014	0.8501 $\pm$ 0.0003	0.7963 $\pm$ 0.0005	0.4101 $\pm$ 0.0053	20.0720 $\pm$ 0.0072	0.2290 $\pm$ 0.0011
RTDL	0.9682 $\pm$ 0.0018	0.8563 $\pm$ 0.0011	0.7936 $\pm$ 0.0004	0.4107 $\pm$ 0.0048	20.0844 $\pm$ 0.0098	0.2317 $\pm$ 0.0034
ResNet	0.8743 $\pm$ 0.0183	0.8361 $\pm$ 0.0144	0.8146 $\pm$ 0.0092	0.3477 $\pm$ 0.0048	18.6150 $\pm$ 1.4559	0.2512 $\pm$ 0.0034
KD	0.8390 $\pm$ 0.0076	0.8382 $\pm$ 0.0063	0.8118 $\pm$ 0.0046	0.3532 $\pm$ 0.0035	19.0683 $\pm$ 1.7642	0.2499 $\pm$ 0.0015
MFH	–	0.8312 $\pm$ 0.0022	0.7507 $\pm$ 0.0034	0.3401 $\pm$ 0.0027	43.1455 $\pm$ 2.0843	0.2873 $\pm$ 0.0047
FMR	0.8427 $\pm$ 0.0151	0.8347 $\pm$ 0.0119	0.8003 $\pm$ 0.0143	0.3526 $\pm$ 0.0088	19.3517 $\pm$ 1.5837	0.2937 $\pm$ 0.0084
MMCL	0.8203 $\pm$ 0.0040	0.8431 $\pm$ 0.0012	0.8041 $\pm$ 0.0017	0.2981 $\pm$ 0.0026	–	–
CHARMS	<b>0.9175<math>\pm</math>0.0052</b>	<b>0.8661<math>\pm</math>0.0032</b>	<b>0.8220<math>\pm</math>0.0022</b>	<b>0.3603<math>\pm</math>0.0037</b>	<b>18.4314<math>\pm</math>0.7427</b>	<b>0.2495<math>\pm</math>0.0025</b>

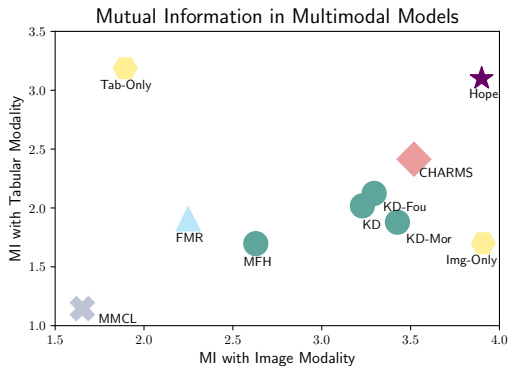


Figure 1: Mutual Information with Different Modality in Multimodal Models. A good model should be able to effectively combine both image and tabular information, resulting in higher mutual information between the two modalities.

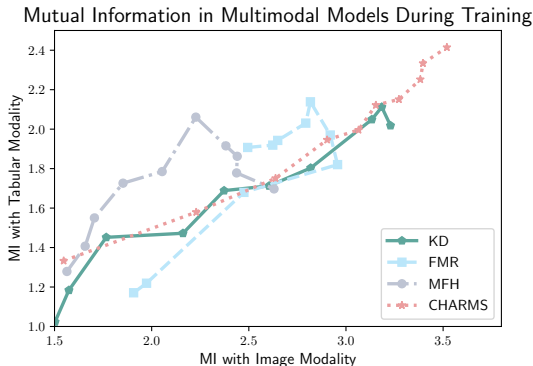


Figure 2: Mutual Information During Training on MVFEAT dataset. We calculate mutual information from the beginning to the convergence process in order to better understand the training process of each method.

98 We experiment on five random seeds and the results in the form of mean plus standard deviation are  
 99 shown in the table 2.

### 100 A.3 Figure Details

101 We explain some figures in detail.

- 102 • For Figure 4, we calculated the amount of information contained in different modality data  
 103 for different methods with the MINE method [1]. The image data are simple handwritten  
 104 digits, we process them simply using a two-layer convolutional neural network, followed  
 105 by a max pooling layer, and a Dropout layer to prevent overfitting. When calculating the  
 106 mutual information, we use the *mine* method as the loss function for approximating the  
 107 mutual information. The network we choose is a three layer MLP with two hidden layers of  
 108 size 100, the method we choose is *concat*, and the *batch\_size* is 16.
- 109 • For Figure 2, we do not calculate the mutual information change process for the MMCL  
 110 method because the MMCL method already performs much less well in Figure 4 than the  
 111 other baseline models. We hypothesize that MMCL maps the tabular and image representa-  
 112 tions to another space and therefore the mutual information is lower.
- 113 • In the ablation study for different nets, we experimentally validated the impact of different  
 114 neural network as backbone models on our approach. The accuracy in ORIGIN is {34.77,  
 115 34.05, 34.49, 33.98}. The accuracy in out CHARMS is {35.74, 35.52, 35.82, 35.45}.

### 116 A.4 Task Details

117 The usage of knowledge from table to images could be explained from three aspects:

118 In our setting, the goal is to transfer knowledge from the tabular data to the image model. Both  
119 classification and regression tasks are vital and commonly encountered in our setting, where both  
120 of them are investigated in our experiments. For instance, on the Adoption dataset, the pet type  
121 and size attributes are crucial for the adoption time classification. Guidance on these features in an  
122 image would lead to better learning of the image model. Similarly, on the Pawpularity dataset, the  
123 eyes and face attributes have a positive assignment on the regression of the popularity of the pet.  
124 Therefore, it makes sense to do knowledge transfer from tabular data to image for both classification  
125 and regression tasks.

126 CHARMS is a general method for both classification and regression tasks, in detail, we use cross  
127 entropy loss for classification task and mean square error loss for regression task. We achieved an  
128 improved image representation by employing the CHARMS method, which leverages the guidance  
129 of tabular data on the image data. Specifically, for the classification task, our approach facilitated  
130 the representation with a more discerning distribution over the target categories. On the other hand,  
131 the regression task enabled us to learn an image representation that better approximated the target  
132 values during prediction. The fact that our method performs well on both tasks underscores its  
133 generalizability and effectiveness.

134 Additionally, our visualization experiments provide further evidence of the effectiveness of our  
135 method. These experiments reveal that the attributes and channels selected by our approach are  
136 appropriately matched, leading to an enhancement in the performance of the image model. This  
137 alignment between the attributes and channels serves as strong evidence that we have successfully  
138 transferred the relevant knowledge from the table to the image model.

139 In summary, our approach demonstrates its versatility by excelling in both classification and regression  
140 tasks, showcasing its ability to enhance image representations using guidance from tabular data.

## 141 **B Analysis on Our CHARMS Method**

### 142 **B.1 Comparison with attention method**

143 Our method employs the transfer matrix obtained by OT to weigh the images, with the weights of the  
144 corresponding channels raised to learn the tabular attributes. An alternative approach is to use the  
145 attention method to weigh the image channels differently and learn each tabular attribute separately,  
146 which is a more intuitive approach:

$$\phi(\mathbf{x}^T)_{att} = \mathcal{T}(\phi(\mathbf{x}^T)) \cdot \phi(\mathbf{x}^T) \quad (1)$$

147 where  $\mathcal{T}$  is a two layer MLP that first downscales the image representation obtained by  $\phi$  before  
148 rescaling it to its original dimension, thereby weighting the different channels of the image.

149 In contrast to our method CHARMS, this method assigns a weight to each input element so that the  
150 model can pay more attention to those input elements that are more important for the task at hand. The  
151 attention method constructs a learnable mask for each attribute and learns each attribute separately  
152 based on the backbone network. However, this approach may result in unequal impacts of different  
153 masks on the main task. In contrast, our method weights the attention of different channels in the  
154 representation obtained by the main task, which essentially corrects the main task while avoiding  
155 potential inconsistency issues caused by the attention method.

156 We compare the performance of our method CHARMS with the attention method in all experiments  
157 and summarized the results in Table 4. The table shows that the attention method did not perform  
158 as well as our method on all datasets. Specifically, on the DVM dataset, which involves a complex  
159 downstream task of 129 classification tasks, the attention method constructed different attentions  
160 for different attributes, which confused the backbone network and led to a decrease in overall task  
161 performance.

162 This finding highlights the impracticality of using the attention mechanism alone to integrate the  
163 abundant information in tabular data into the image model. This further supports the effectiveness of  
164 our proposed approach.

Table 3: Comparison with CLIP method. Here CLIP-LP means two encoders are fixed, and only the classification head is trained. CLIP-FT means fine-tuning the entire CLIP network.

	DVM $\uparrow$	SUN $\uparrow$	CelebA $\uparrow$	Adoption $\uparrow$	Pawpularity $\downarrow$	Avito $\downarrow$
CLIP-LP	0.7619	0.6918	0.7590	0.3047	20.1537	0.2972
CLIP-FT	0.8417	0.8333	0.8165	0.2935	42.9489	0.2940
CHARMS	<b>0.9175</b>	<b>0.8661</b>	<b>0.8220</b>	<b>0.3603</b>	<b>18.4314</b>	<b>0.2495</b>

Table 4: Comparison with Attention method. Here Attention means we directly conduct the attention mechanism on the feature extracted by  $\phi$  and learn an attention mask for all tabular attributes.

	DVM $\uparrow$	SUN $\uparrow$	CelebA $\uparrow$	Adoption $\uparrow$	Pawpularity $\downarrow$	Avito $\downarrow$
Attention	0.4757	0.8550	0.8180	0.3454	18.7401	0.2544
CHARMS	<b>0.9175</b>	<b>0.8661</b>	<b>0.8220</b>	<b>0.3603</b>	<b>18.4314</b>	<b>0.2495</b>

165 **B.2 Comparison with CLIP method**

166 CLIP is pre-trained on a large amount of text and image pairs, which makes it able to map from  
 167 text to images. Some previous studies have demonstrated that CLIP is able to transform tabular data  
 168 to text for classification given the column names [15, 4]. However, CLIP is heavily reliant on the  
 169 semantic information contained within the text, so that the semantics of attributes are inevitable.

170 Indeed, the setting of this paper is more general. We expect to transfer the tabular knowledge to the  
 171 image modality during training to cope with the absence of expert knowledge during testing. Our  
 172 method CHARMS aims to automatically extract the semantic information from the tabular and align it  
 173 with the corresponding image channels without requiring explicit knowledge of the attribute’s precise  
 174 meaning. Specifically, as we show in Section 4.2, based on measuring the similarity across attributes  
 175 and channels, OT discovers and aligns the attribute semantic automatically.

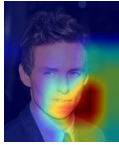




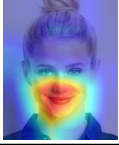

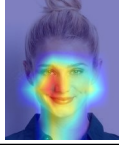
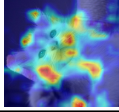
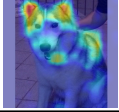
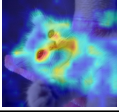
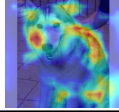


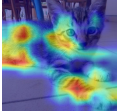
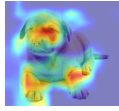
176 We conducted an experiment with CLIP. In this experiment, we converted the tabular data into text  
 177 format, such as "length: 16". To ensure a fair comparison, we utilized CLIP from ?? with the  
 178 ResNet50 backbone. The CLIP model consists of an image encoder and a textual encoder, and  
 179 we connected a one-layer linear head for classification or regression after the image encoder. Two  
 180 versions of CLIP were trained in our experiment. CLIP-LP means CLIP-LinearProb, which denotes  
 181 the scenario where the two encoders are fixed, and only the classification head is trained. CLIP-FT  
 182 means CLIP-FineTune, on the other hand, involves fine-tuning the entire CLIP network. With the  
 183 contrastive learning of the two modalities of the CLIP model, tabular knowledge is transferred to the  
 184 image modality. By transforming the task into a language-to-vision knowledge transfer, the results  
 185 were obtained in table 3.

186 From the experiments, we can see that the performance of CLIP is not ideal. This is probably due  
 187 to the fact that in tabular data, each column holds its own distinct meaning, and directly utilizing it  
 188 as input to CLIP can lead to the loss of certain information. For instance, on the CelebA dataset,  
 189 the attribute "wood (not part of a tree)" might not be a highly significant feature. However, when  
 190 this attribute is converted to text format, its character length tends to be relatively long, which can  
 191 introduce redundancy in the information.

192 From another perspective, previous work has pointed out that there is a modality gap in the CLIP’s  
 193 embedding space [7]. This gap is caused by a combination of model initialization and contrastive  
 194 learning optimization. In a multi-modal model with two encoders, the representations of the two  
 195 modalities are clearly apart when the model is initialized. During optimization, contrastive learning  
 196 keeps the different modalities separate by a certain distance. This gap makes the CLIP method fail in  
 197 our task.

198 In summary, the loss of information and the modality gap that arises when transferring tabular data  
 199 to images can hinder the performance of the CLIP method in our setting. However, our method  
 200 addresses these challenges by automatically discovering and establishing the matching relationship  
 201 between the two modalities, thereby facilitating effective knowledge transfer, which is a more general  
 202 method.

Table 5: More Visualization by GradCAM.

Tabular Attribute	5_o_Clock_Shadow	Arched_Eyebrows	Big_Nose	Blond_Hair
Aligned Channel	65, 87, 119, 236...	33, 76, 78, 115, ...	50, 224, 258, ...	684
Visualization				
Tabular Attribute	High_Cheekbones	Smiling	Oval_Face	Rosy_Cheeks
Aligned Channel	2, 26, 41, 85,...	11, 12, 28, 57, ...	52, 646, 924, ...	4, 47, 88,...
Visualization				
Tabular Attribute	Type		Color	
Aligned Channel	399, 413, 414, 521...		400, 412, 425, 448...	
Visualization				
Aligned Channel	399, 413, 414, 521...		400, 412, 425, 448...	
Visualization				

## 203 C More Experiments

### 204 C.1 More Visualization

205 We provide more visualizations in Table 5 to validate the ability of CHARMS to match the correspond-  
 206 ing attributes and channels. We apply GradCAM on various datasets, which show similar visualization  
 207 results, where the channels could be matched to a certain attribute with semantic meaning.

208 For the Adoption dataset, all tabular attributes are inherently more abstract in nature. However, for  
 209 the purpose of visualization, we have specifically selected features that are visually recognizable by  
 210 humans from images. For instance, attributes such as the type of pet and the color of the pet highlight  
 211 more general aspects that are of interest.

212 From the visualization, we can see that the judgment of the pet type focuses more on the pet’s head,  
 213 whereas the judgment of the color takes into account the whole body of the pet, and from this point  
 214 of view we believe that our approach does achieve knowledge transfer.

### 215 C.2 Visualization with t-SNE

216 To visualize the impact of our method on the distribution of image features, we conducted experiments  
 217 using the t-SNE method [14]. t-SNE can map high-dimensional data to a two- or three-dimensional  
 218 space, enabling better visualization and interpretation of the data structure. The method employs a  
 219 nonlinear mapping approach that minimizes the difference between the distances of points in high-  
 220 dimensional space and those in low-dimensional space. Specifically, it represents high-dimensional  
 221 data points as probability distributions and generates corresponding probability distributions in the  
 222 low-dimensional space. Then, it uses KL divergence to measure the difference between the two  
 223 probability distributions and minimizes it to achieve the best mapping effect.

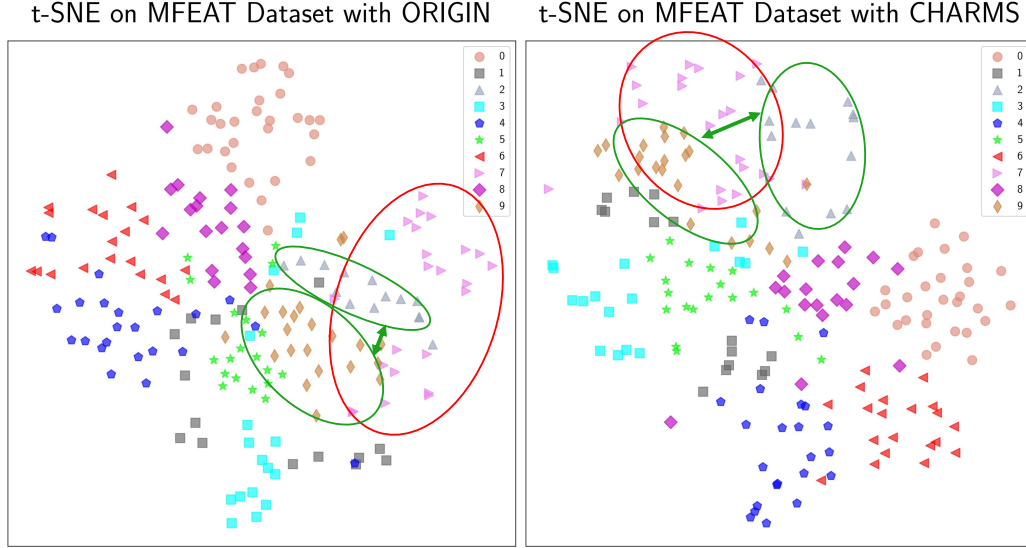


Figure 3: Visualization of t-SNE on the MFEAT dataset. the ORIGIN method represents training on image modalities only. As can be seen from the figure, our method makes the intra-class distance smaller and the inter-class distance larger. Therefore the transfer of expert knowledge from tabular data to the image model is effective. The red circles mean that our method makes the intra-class distance smaller, and the green circles indicate that our method makes the inter-class distance larger.

224 The experimental results are presented in Figure 3, where the ORIGIN method refers to training with  
 225 image modalities only. The figure shows that the ORIGIN method achieved good segmentation results  
 226 due to the task’s simplicity. However, due to the lack of expert knowledge, the intra-class distance is  
 227 still large, particularly for samples with label 7, while the inter-class distances remain small, such  
 228 as for samples with labels 2 and 9. In contrast, our method compensates for these deficiencies by  
 229 transferring expert knowledge.

### 230 C.3 More Mutual Information experiments

231 We chose the MFEAT dataset for the Mutual Information experiments since, in this dataset, the  
 232 formal features of each category are simple and easily distinguishable. For example, morphological  
 233 features and non-morphological features. And the images are all digital images, which are relatively  
 234 simple and easy to understand. The experiment mainly helps us understand. More mutual information  
 235 experiments can be obtained in Table 4 5.

236 The experiments in PetFinder-adoption dataset also indicate that existing methods for transferring  
 237 tabular knowledge to image models yield low mutual information between the representations and  
 238 tabular data. Our CHARMS method, on the other hand, maximises the mutual information of tabular  
 239 and images to achieve better results.

### 240 C.4 More Ablation Studies

241 In the CHARMS method, we use the K-Means [9, 10] method to cluster the 2048-dimensional features  
 242 extracted from ResNet. We discuss the number of clusters on the SUNAttribute dataset, and the  
 243 results in Table 6 show that the performance of CHARMS is not affected by the number of clusters  
 244 taken, demonstrating the robustness of the method to hyperparameter choices. This robustness  
 245 makes the method more flexible and reliable in practical applications, as it does not require excessive  
 246 hyperparameter tuning or fine-tuning, saving time and effort.

247 To further demonstrate the applicability and robustness of our proposed method, CHARMS, we  
 248 conducted experiments using different network structures on DVM dataset with results shown in  
 249 Table 7. The result also shows that the performance improvements achieved by our method are  
 250 consistent across different network structures.



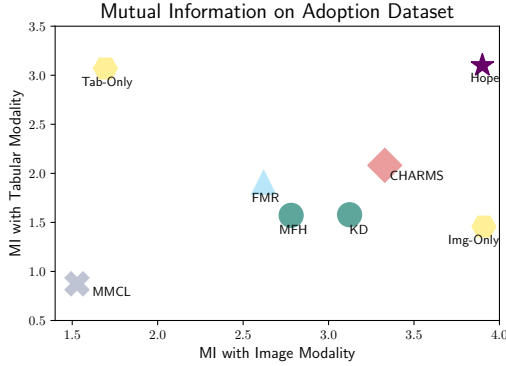


Figure 4: Mutual Information with Different Modality on the Adoption Dataset.

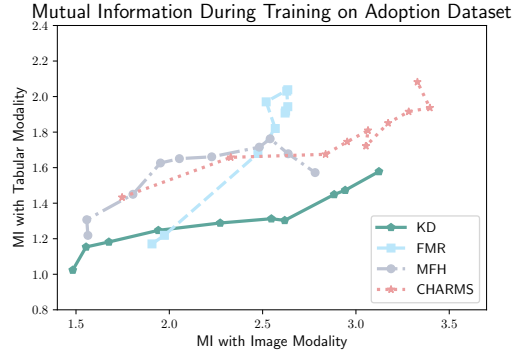


Figure 5: Mutual Information During Training on the Adoption dataset.

Table 6: Ablation study on cluster number on SUNAttribute dataset.

n_cluster	20	40	60	80	100
Accuracy	0.8494	0.8661	0.8494	0.8556	0.8522

## 251 D Limitations and Future Works

252 Our approach relies on leveraging mutual information between the two modalities, which establishes  
 253 the feasibility of knowledge transfer. When there is a significant amount of mutual information  
 254 present between the tabular and image modalities, our approach can effectively transfer relevant  
 255 knowledge and insights between them. On the other hand, converting text into tables is indeed a  
 256 viable approach, but this approach results in the loss of some of the textual information and it is  
 257 challenging to handle such a conversion well. The problem of testing data drift also exists in real life.  
 258 We will consider this problem deeply in future work. In terms of social impact, we think that our  
 259 approach holds potential for application in the medical field, where it can assist doctors in making  
 260 rapid and accurate diagnoses. There should be no negative social impact of our method.

261 Our work demonstrates the effectiveness of our method in both classification and regression tasks. In  
 262 future work, it would be valuable to investigate the applicability of our method to other tasks, such  
 263 as semantic segmentation. These types of tasks may require additional domain-specific knowledge,  
 264 such as precise object localization within images, to achieve optimal performance. Nonetheless, we  
 265 believe that our approach is still applicable for such tasks.

266 On the other hand, the high cost of annotating expert data often leads to imbalanced datasets, which  
 267 pose a challenge for improving image model performance using a limited amount of tabular data.  
 268 Therefore, addressing this data imbalance is crucial for future work.

## 269 References

- 270 [1] Mohamed Ishmael Belghazi, Aristide Baratin, Sai Rajeswar, Sherjil Ozair, Yoshua Bengio,  
 271 Aaron Courville, and R Devon Hjelm. Mine: mutual information neural estimation. *arXiv*  
 272 *preprint arXiv:1801.04062*, 2018.

Table 7: Impact of different network structures on the method on DVM dataset.

	ResNet	DenseNet	Inception	MobileNet
Model Size / M	25.8	8.2	6.8	3.7
ORIGIN	0.8743	0.8671	0.7492	0.8206
CHARMS	0.9175	0.9115	0.9012	0.8961

- 273 [2] Yury Gorishniy, Ivan Rubachev, Valentin Khruikov, and Artem Babenko. Revisiting deep  
274 learning models for tabular data. *Advances in Neural Information Processing Systems*, 34:18932–  
275 18943, 2021.
- 276 [3] Paul Hager, Martin J Menten, and Daniel Rueckert. Best of both worlds: Multimodal contrastive  
277 learning with tabular and imaging data. *arXiv preprint arXiv:2303.14080*, 2023.
- 278 [4] Stefan Hegselmann, Alejandro Buendia, Hunter Lang, Monica Agrawal, Xiaoyi Jiang, and  
279 David Sontag. Tabllm: Few-shot classification of tabular data with large language models. In  
280 *International Conference on Artificial Intelligence and Statistics*, pages 5549–5581, 2023.
- 281 [5] Geoffrey Hinton, Oriol Vinyals, and Jeff Dean. Distilling the knowledge in a neural network.  
282 *arXiv preprint arXiv:1503.02531*, 2015.
- 283 [6] Jingmin Huang, Bowei Chen, Lan Luo, Shigang Yue, and Iadh Ounis. Dvm-car: A large-scale  
284 automotive dataset for visual marketing research and applications. In *2022 IEEE International  
285 Conference on Big Data*, pages 4140–4147, 2022.
- 286 [7] Victor Weixin Liang, Yuhui Zhang, Yongchan Kwon, Serena Yeung, and James Y Zou. Mind  
287 the gap: Understanding the modality gap in multi-modal contrastive representation learning.  
288 *Advances in Neural Information Processing Systems*, 35:17612–17625, 2022.
- 289 [8] Ziwei Liu, Ping Luo, Xiaogang Wang, and Xiaoou Tang. Deep learning face attributes in the  
290 wild. In *Proceedings of International Conference on Computer Vision*, pages 3730–3738, 2015.
- 291 [9] Stuart Lloyd. Least squares quantization in pcm. *IEEE transactions on information theory*,  
292 28:129–137, 1982.
- 293 [10] J MacQueen. Classification and analysis of multivariate observations. In *5th Berkeley Symp.  
294 Math. Statist. Probability*, pages 281–297, 1967.
- 295 [11] Genevieve Patterson, Chen Xu, Hang Su, and James Hays. The sun attribute database: Beyond  
296 categories for deeper scene understanding. *International Journal of Computer Vision*, 108:59–81,  
297 2014.
- 298 [12] Olga Russakovsky, Jia Deng, Hao Su, Jonathan Krause, Sanjeev Satheesh, Sean Ma, Zhiheng  
299 Huang, Andrej Karpathy, Aditya Khosla, Michael Bernstein, et al. Imagenet large scale visual  
300 recognition challenge. *International journal of computer vision*, 115:211–252, 2015.
- 301 [13] Martijn van Breukelen, Robert PW Duin, David MJ Tax, and JE Den Hartog. Handwritten digit  
302 recognition by combined classifiers. *Kybernetika*, 34:381–386, 1998.
- 303 [14] Laurens Van der Maaten and Geoffrey Hinton. Visualizing data using t-sne. *Journal of machine  
304 learning research*, 9(11), 2008.
- 305 [15] Zifeng Wang and Jimeng Sun. Transtab: Learning transferable tabular transformers across  
306 tables. *arXiv preprint arXiv:2205.09328*, 2022.
- 307 [16] Zihui Xue, Zhengqi Gao, Sucheng Ren, and Hang Zhao. The modality focusing hypothesis:  
308 Towards understanding crossmodal knowledge distillation. *arXiv preprint arXiv:2206.06487*,  
309 2022.
- 310 [17] Yang Yang, De-Chuan Zhan, Ying Fan, Yuan Jiang, and Zhi-Hua Zhou. Deep learning for  
311 fixed model reuse. In *Proceedings of the AAAI Conference on Artificial Intelligence*, pages  
312 2831–2837, 2017.